TEMPORAL E-BEAM SHAPING IN AN S-BAND ACCELERATOR

H. Loos*, D. Dowell, S. Gilevich, C. Limborg-Deprey, SLAC, Menlo Park, CA 94025, USA
Y. Shen, J. Murphy, B. Sheehy, T. Tsang, X. Wang, Z. Wu, BNL, Upton, NY 11973, USA
L. Serafini, INFN-Milano, Milan, Italy
M. Boscolo, M. Ferrario, M. Petrarca, C. Vicario, INFN/LNF, Frascati (Rome), Italy

Abstract

New short-wavelength SASE light sources will require very bright electron beams, brighter in some cases than is now possible. One method for improving brightness involves the careful shaping of the electron bunch to control the degrading effects of its space charge forces. We study this experimentally in an S-band system, by using an acousto-optical programmable dispersive filter to shape the photocathode laser pulse that drives the RF photoinjector. We report on the efficacy of shaping from the IR through the UV, and the effects of shaping on the electron beam dynamics.

INTRODUCTION

The experiments reported here were conducted at the DUV-FEL facility at BNL/NSLS with a suitable photo injector and drive laser in collaboration with the SPARC Project at INFN-LNF providing the acousto-optical programmable dispersive filter (AOPDF) used to temporally shape the laser pulses.

The DUV-FEL facility [1] consists of a frequency tripled Ti:Sapphire amplifier laser, a 250 MeV S-band accelerator, and the NISUS undulator for SASE and High Gain Harmonic Generation FEL experiments in the IR and deep UV [2]. The accelerator features a 6 MeV BNL/SLAC/UCLA gun, 2 SLAC-type accelerating structures providing 70 MeV followed by a 4 dipole chicane and three more accelerating structures with a final energy of up to 250 MeV after a recent energy upgrade [3]. A spectrometer dipole after the last structure enables energy spectra and time resolved measurements [4].

The first part of this paper describes the laser system and the pulse shaping method. The second part reports on the measurements of the electron beam properties using shaped drive laser pulses.

LASER SHAPING

The principle of an AOPDF [5] is to generate an acoustic wave in a birefringent crystal (tellurium oxide) which diffracts the incident light wavelength dependent. The small scaling factor $\alpha = \Delta n\ V/c$ (acoustic speed V and index difference Δn) of typically 10^{-7} between the acoustic and optic wave allows the diffraction of 800 nm light with a 50 MHz rf signal. In frequency domain, the diffracted light wave is $E_{out}(\omega) = E_{in}(\omega)\ S(\alpha\omega)$ with an acoustic wave $S(\omega)$, thus allowing arbitrary modulations of phase and amplitude within the temporal limits given by the crystal length.

The DUV-FEL photocathode laser system is shown in Fig. 1. A 5 W green Millenia V laser pumps a 10 nJ, 100 fs Ti:Saphhire oscillator. The oscillator pulse is stretched to 200 ps and amplified in a flash-lamp YAG pumped regenerative oscillator to 2 mJ and in a 2-pass amplifier to 20 mJ. After a grating compressor 9 mJ remaining infrared are doubled and tripled in a 500 μm and a 100 μm BBO crystal giving 500 μJ of UV light. A spatial filter consisting of a pin-hole and an iris aperture reduces the UV to 50 μJ being sent to the photo-cathode.

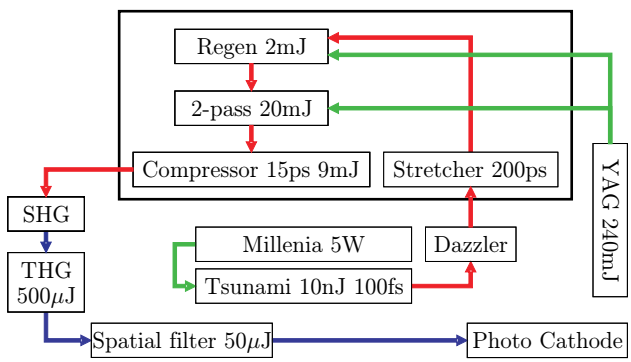

Figure 1: Layout of the DUV-FEL laser system including the DAZZLER.

The AOPDF (a DAZZLER from FASTLITE) was inserted behind the Ti:Sa oscillator considering the damage threshold of the device. At that location the pulse shape of the final UV pulse will be affected by both the amplification and the harmonic conversion process, which has to be taken into account to find the appropriate amplitude and phase filter for the AOPDF.

Laser Diagnostics

Both spectral and temporal diagnostics were used to characterize the 800, 400, and 266 nm light. Single shot and averaged spectra were obtained with a monochromator using an 1800/mm grating. The SHG and THG light spectra were taken in second and third order. Time distributions at all wavelengths were obtained with a streak camera with 2 ps resolution in synchro-scan mode and with a scanning cross-correlator for the UV light with a resolution of 200 fs.

* loos@slac.stanford.edu

Shaping Results

The goal of the study was to generate a 10 ps long flat-top UV laser pulse with a 1 ps rise/fall time and a flatness of 10%. These parameters were shown to be optimal in a similar experiment using an LCSLM [6]. Three different methods were pursued to obtain the proper filter for the AOPDF. The first strategy relied on the time-wavelength correlation of a chirped pulse in creating a 10th order super-gaussian spectrum which corresponds to a nearly flat-top time distribution within the requirements. To account for the saturation effect in the amplifier, a few iterations were necessary, in which the ratio between the actual spectrum and the goal spectrum was used as a multiplicative correction to the amplitude filter of the AOPDF. The second method was the implementation of a genetic algorithm to optimize the time shape directly. Simulations showed good conversion after several hundred iterations. However, the fact that no single shot measurement with high resolution was available, made this method unfeasible. The third method was to manually tune amplitude and phase of the filter function.

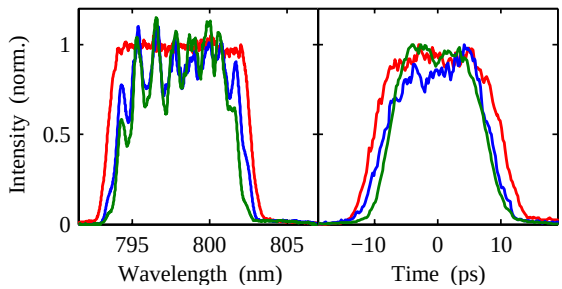

Figure 2: Spectra and streak camera time profiles of 15 ps long shaped laser pulse.

The results of the iterative spectrum optimization are shown in Figs. 2 and 3. The incident 10 nm wide Gaussian oscillator spectrum was shaped into a 9 nm wide flat-top IR spectrum. The slight loss of bandwidth in the blue light is due to the bandwidth limitation of the 500 μm thick SHG crystal. An even larger loss in the UV bandwidth could be prevented by replacing the original 250 μm crystal with a 100 μm thick one. The time distributions from the streak camera show a corresponding shortening between the IR and the blue. The comparison of the high resolution cross-correlation and the UV spectrum exhibit a strong correlation between the spectral and the temporal modulation. The source of this modulation was found to be the stretcher and the regenerative amplifier. Further experiments confirmed that small amplitude modulations in the oscillator pulse eventually create large modulations in the UV spectrum with a gain of about 10. The mechanism is presumably a Kerr-effect in the regenerative amplifier crystal which converts amplitude into phase modulation. This phase modulation becomes apparent only in the spectra of the generated harmonics and also produces temporal modulation.

Since the spectral phase changes are not influenced by the amplification process, the Kerr-induced phase modulations could in principle be corrected with a phase filter for the AOPDF. However, the modulation period of about 1 nm is too fine considering the effective resolution of the Dazzler of 1 nm. Furthermore, the modulation amplitude was fluctuating up to 50% from shot to shot due to small variations in the saturation power of the regen and thus limiting the ability to suppress the modulation.

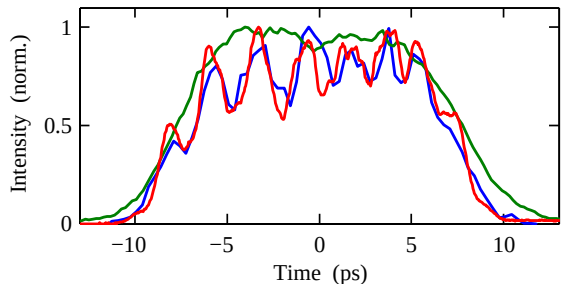

Figure 3: Time profile of 15 ps long shaped UV laser pulse. The blue line shows the cross-correlation, the green the streak camera, and the red the UV spectrum scaled to match the time distribution.

To produce the required 10 ps UV pulse for the photoinjector, the IR pulse was shortened in the studies with the electron beam. The resulting UV pulse was 8 ps long with 1 ps long edges, but 30% variation throughout the pulse.

ELECTRON BEAM MEASUREMENTS

The electron beam was generated with the gun phase at 30° and both phases of linac 1 and 2 set to maximize the energy to 65 MeV and to minimize residual chirp. The following chicane was not powered to measure the uncompressed beam. Electron beam images were generated at various YAG screens and measured with CCD cameras. The projected transverse emittances were measured using three screens along linacs 3 and 4, which were not powered then. Time resolved measurements were taken at the screen after the spectrometer dipole with linac 3 or 4 set to zero phase to impose a known, variable chirp to the beam. The time resolved vertical slice emittance was obtained by vary-

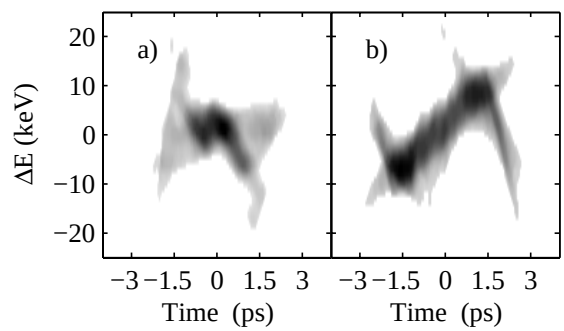

Figure 4: Longitudinal phase space reconstructions for 70 pC. Panel a) shows the Gaussian, b) the flat-top case.

ing a quadrupole upstream of the spectrometer to generate a vertical focus and correlating the horizontal energy distribution of the beam to a time coordinate with the known chirp. The longitudinal phase space parameters were measured by varying the sign and amplitude of the chirp while recording the energy distribution. Analyzing the energy spread gives the longitudinal emittance and bunch length, whereas a tomographic reconstruction [7] using the energy profiles resolves the phase space distribution and thus the energy time correlation and the beam current distribution.

The experiments were done for bunch charges of 70 pC and 300 pC and an non-shaped Gaussian and a shaped flat-top UV laser pulse. The filter for the AOPDF was manually tuned to minimize the modulation in the laser pulse by monitoring the modulation in the energy spectrum of the electron beam. The reconstructed longitudinal phase space for the low charge case is shown in Fig. 4, the corresponding slice energy deviation and the electron and laser beam time distributions are displayed in Fig. 5. The vertical slice emittance and the beam mismatch parameter $\xi = (\gamma_0\beta - 2\alpha_0\alpha + \beta_0\gamma)/2$ are shown in Fig. 6. The Twiss parameters of the central slice were used as reference for the mismatch.

Table 1: Laser and electron beam parameters

Shaped			No	Yes	No	Yes
Charge		pC	70	70	300	300
Laser σ_z	rms	ps	2.0	2.7	2.0	2.8
Laser σ_z	fwhm	ps	4.8	7.8	4.8	7.5
σ_z		ps	1.15	1.43	1.7	1.9
ΔE	proj	keV	5.7	8.0	5.1	6.8
$\epsilon_{z,n}$		μm	5.5	8.1	10	15
ΔE	ave	keV	4.3	4.0	4.3	7.0
$\Delta E/E$	ave	10^{-5}	7	6	7	10
$\epsilon_{y,n}$	proj	μm	1.7	1.4	2.0	1.5
Matched Charge		pC	42	50	217	270

The electron beam and corresponding laser parameters obtained from these measurements are listed in Table 1. The average energy spread values are taken over all slices disregarding the correlation which increases the projected values. The matched charge value is the amount of charge with a mismatch parameter of less than 1.15. The projected vertical emittance in the low charge case was calculated from the slice measurement, whereas the numbers at high charge are from the three screen measurement. In both cases, a significant reduction of vertical emittance could be observed due to the shaping of the laser, which is due to a better slice alignment.

SUMMARY

The desired pulse length and rise time of the UV laser pulse could be obtained by using an AOPDF for shaping. The lack of a fast temporal diagnostic made the optimization of the required flatness unfeasible. The electron beam with the shaped laser had a more uniform longitudinal phase space, a reduced projected transverse emittance, and a larger part of the pulse with matched slices.

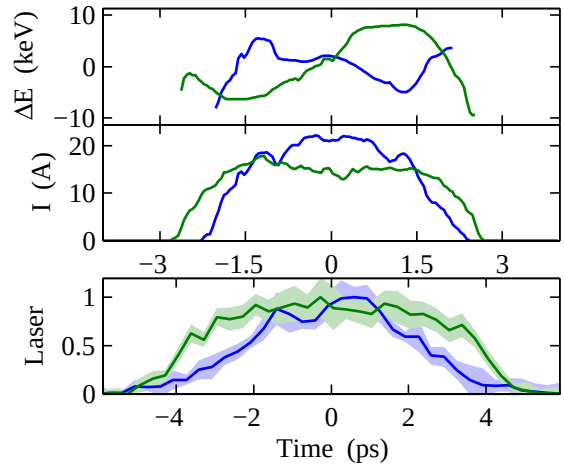

Figure 5: Time distributions from phase space reconstruction. Blue indicates the Gaussian, green the flat-top case. The top panel shows the correlation between slice energy vs. time, the middle shows the current distribution, and the bottom the corresponding UV laser pulse distributions.

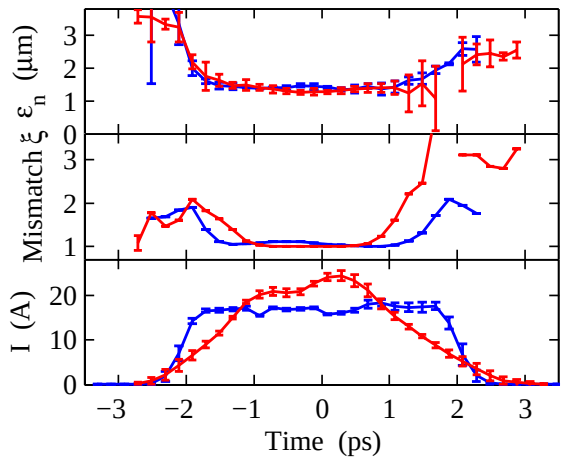

Figure 6: Vertical slice emittances for 70 pC. Red indicates the Gaussian, blue the flat-top case.

This work was supported by DOE Contracts DE-AC03-76SF00515 and DE-AC02-98CH10886.

REFERENCES

[1] W. S. Graves et al., PAC 2001, Chicago, June 2001, p. 2860
[2] L.H. Yu et al., Phys. Rev. Lett. **91** (2003) 074801
[3] X.J. Wang et al., these proceedings, TOAB003
[4] W. S. Graves et al., PAC 2001, Chicago, June 2001, p. 2224
[5] F. Verluise et al., Opt. Lett. **25** (2000) 575
[6] J. Yang et al., EPAC 2002, Paris, June 2002, p. 1828
[7] H. Loos et al., Nucl. Instrum. Meth. A 528 (2004) 189